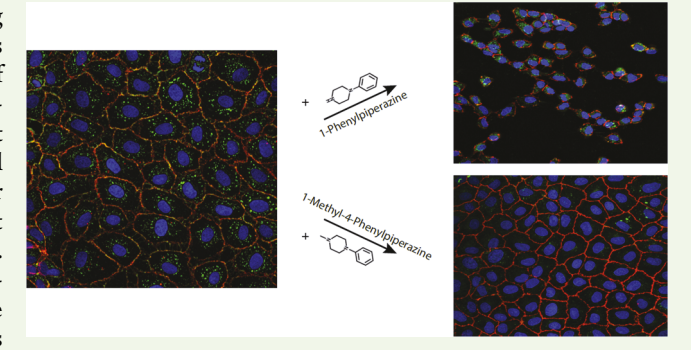


Piperazine Derivatives Enhance Epithelial Cell Monolayer Permeability by Increased Cell Force Generation and Loss of **Cadherin Structures**

Shiyuan Zheng,^{†,||} Kirill Lavrenyuk,^{§,||} Nicholas G. Lamson,[‡] Katherine C. Fein,[‡] Kathryn A. Whitehead,[‡] and Kris Noel Dahl*,^{†,‡,§}

Supporting Information

ABSTRACT: A major obstacle for topical and enteral drug delivery is the poor transport of macromolecular drugs through the epithelium. One potential solution is the use of permeation enhancers that alter epithelial structures. Piperazine derivatives are known permeation enhancers that modulate epithelial structures, reduce transepithelial electrical resistance, and augment the absorption of macromolecular drugs. The mechanism by which piperazine derivatives disrupt the structures of epithelial monolayers is not well understood. Here, the effects of 1-phenylpiperazine and 1-methyl-4phenylpiperazine are modeled in the epithelial cell line NRK-52E. Live-cell imaging reveals a dose-dependent gross reorganization of monolayers at high concentrations, but



reorganization differs based on the piperazine molecule. Results show that low concentrations of piperazine derivatives increase myosin force generation within the cells and do not disrupt the cytoskeletal structure. Also, cytoskeletally attached cadherin junctions are disrupted before tight junctions. In summary, piperazines appear to increase myosin-mediated contraction followed by disruption of cell-cell contacts. These results provide new mechanistic insight into how transient epithelial permeation enhancers act and will inform of the development of future generations of transepithelial delivery systems.

KEYWORDS: permeation enhancer, mechanobiology, epithelial permeability, oral delivery, cell structure

INTRODUCTION

Drug delivery across epithelial barriers offers improved convenience and patient compliance compared to injection. However, drug transport across gastrointestinal and lung epithelial barriers has historically been limited to small molecules. Currently, the U.S. Food and Drug Administration has approved only two peptides for oral dosing for systemic delivery, both of which are <2000 g/mol. The delivery of larger therapeutic proteins (e.g., ~150,000 g/mol for antibodies) remains a challenge. Macromolecular drugs face a series of barriers in epithelial spaces; for the intestinal epithelium, these barriers include a mucus layer on the apical surface of the epithelium and protein complexes called tight junctions in the paracellular space between adjacent intestinal epithelial cells.² Several strategies have been developed to augment the absorption of macromolecular drugs through epithelial monolayers including complexation with bioadhesive nanoparticles, delivery agents that form a complex with the protein drug to increase oral bioavailability,4 and promoting a receptormediated transcellular route.⁵ One potential approach ad-

dressed here uses permeation enhancers, which modify the structure of the epithelium or individual cells to increase the permeability of macromolecules across the intestinal epithelium.6

Previous studies by our group and others suggest that a family of molecules called piperazines hold promise as permeation enhancers for the epithelium. 7-10 Piperazines are a broad class of pharmacologically active molecules with six-membered rings and two opposing nitrogens. 11 These molecules were originally developed to treat parasitic infections, and decades of study have produced many piperazine derivatives, which have been further evaluated for toxicity, side effects, and efficacy of specific nonhelmintic functions. From the piperazine library, 1-phenylpiperazine (1ppz) and 1-methyl-4-piperazine (1M4ppz) stand out among piperazine derivatives for their low toxicity and high potency in transepithelial permeation enhancement. However,

Received: November 1, 2019 Accepted: December 2, 2019 Published: December 2, 2019



[†]Department of Biomedical Engineering and [‡]Department of Chemical Engineering, Carnegie Mellon University, 5000 Forbes Avenue, Pittsburgh, Pennsylvania 15213, United States

[§]Molecular Biophysics and Structural Biology, University of Pittsburgh and Carnegie Mellon University, 3501 Fifth Avenue, Pittsburgh, Pennsylvania 15260, United States

the cellular mechanisms by which epithelial cells are modulated by piperazine derivatives to cause permeation of the epithelium layer are not fully elucidated. The study of Bzik and Brayden showed that 1-phenylpiperazine increased the transport of paracellular flux markers across Caco-2 cell monolayers and also mediated tight junctions with acceptable levels of tissue damage. Additionally, Fein and colleagues showed that piperazine derivatives remodeled the Caco-2 epithelial tight junction with relatively low cytotoxicity while enhancing permeation efficiency.

While most mechanistic studies of epithelial permeation enhancers have relied on biochemical analysis, we sought to augment our understanding of piperazine derivatives through topological studies.¹² Therefore, this study focuses on cellular responses, structural characterization, and material properties of epithelial cell monolayers following piperazine derivative treatment. We utilize the model kidney epithelial line NRK-52E for imaging and complement these studies with permeability studies in Caco-2 intestinal epithelial cells. To measure the mechanical response within cells, a particle tracking technique, sensors from intranuclear kinetics (SINK), is used to detect cellular force propagation from collective myosin motors transmitted through the LINC complex (Linkers of Nucleus to Cytoskeleton) and into chromatin. Here, we use the SINK method to measure the force response in model epithelial monolayers and investigate the permeation-enhancing effects of piperazine derivatives. The SINK technique has enabled visualization of the mechanical reorganization of epithelial cells in response to two piperazine derivatives and the comparison of permeation enhancement behavior.

EXPERIMENTAL MATERIALS AND METHODS

Cell Culture and Live-Cell Imaging. NRK-52E epithelial cells [American Type Culture Collection (ATCC)] were cultured in DMEM high-glucose medium supplemented with 5% calf serum and 1% penicillin-streptomycin (Life Technologies). Culture and live imaging of NRK-52E were both performed at 5% CO₂ and 37 °C. For all imaging experiments, the cells were cultured to confluence on coverslip-bottom, 35 mm imaging dish (Ibidi 81218). Caco-2 cells (ATCC) were cultured in DMEM supplemented with 10% FBS, 100 IU/mL penicillin, 0.1 mg/mL streptomycin, and 0.25 μ g/mL amphotericin B (Life Technologies). Cultures were incubated at 37 °C in a fully humid, 5% CO₂ environment. The cells were subcultured with 0.25% trypsin-EDTA and subsequently passaged every 3 to 4 days at ratios between 1:3 and 1:8. Differentiation was performed in Corning HTS 1.0 µm porous support Transwell plates using sodium butyrate and MITO+ serum extender from VWR. Cells at passage numbers 20-50 were utilized for further experiments. The free-to-use PS power calculator (Vanderbilt) was used to determine the minimal sample size for which statistical power was greater than or equal to 0.8 and n = 3 for Caco-2-based experiments.

Piperazines for the Study. 1-Phenylpiperazine (1ppz) was purchased from Sigma Aldrich and 1M4ppz (1-methyl-4-phenylpiperazine) from Ontario Chemicals and were chosen for the study based on their efficacy in intestinal permeability. Stocks were maintained at 6.34 M in sterile DMEM until use.

Live Imaging of NRK-52E Monolayer Disruption. Cells were incubated with calcein AM and Hoechst 33342 (Thermo Fisher) for 30 min in the incubator after which the cells were washed with phosphate-buffered saline (PBS) and the medium was changed. The medium was then added with propidium iodide (PI) and 1-phenylpiperazine at 1, 3, and 10 mM or 1-methyl-4-phenylpiperazine at 1, 3, 10, and 30 mM, and cells were imaged at 20× magnification (0.4 NA) on a DMI6000 (Leica). To measure "cell death" over time, the numbers of live cells (labeled by calcein) and dead cells (labeled by propidium iodide) were compared per image over time by using Fiji ImageJ. Also, "fraction

surface coverage" was determined by the area of the image covered by calcein fluorescence. For each condition, three parallel experiments were conducted and averaged.

Live Imaging of Cytoskeleton and Cellular Fluctuation. To visualize the actin cytoskeletal structure, cells were plated into Ibidi dishes and transfected with RFP-LifeAct plasmids (Ibidi) using Lipofectamine 3000 (Thermo Fisher) as per the manufacturer's recommendations. After 24 h transfection, cells were washed with PBS. The image sequences were acquired at 3 min time intervals for 3 h, with a 63×, 1.4 NA, oil immersion objective on a DMI6000. For live imaging of the actin cytoskeleton, the projected area of an individual cell was measured by using Fiji ImageJ. For each condition, five parallel experiments were conducted and averaged to the final result.

SINK Method. Cells were transfected with the GFP-tagged upstreaming binding factor (GFP-UBF) plasmids using Lipofectamine 3000 (Thermo Fisher). Cells were imaged at 3 min time interval for 1 h with 63×, 1.4 NA, oil immersion on a DMI6000. Cells were imaged at 1 h after image sequencing to guarantee cell viability post imaging. Hoechst 33342 was used to identify the location of the nucleus in a cell. Image analysis was performed as described previously. ^{14,15} Generally, to ensure that GFP-UBF is focused through, only nuclei with proper *z* axis values were selected for analysis. Then, nuclei were taken out from the cytoplasmic background, and the rotation or shift of nuclei was removed; only the intranuclear motion of GFP-UBF spots were tracked and analyzed. Mean squared displacement (MSD) of selected GFP-UBF was calculated versus the lag time τ . In a previous study, our laboratory has shown that, at this sample speed, the MSD of GFP-UBF can be fit to a power-law equation MSD = $D_{\rm eff} \tau^{0}$, where β represents the force generation of the myosin within the cell. ¹⁴

Immunofluorescence. Cells were plated into Millicell Sigma 8wells or 4-wells and grown to confluence. After cells reach confluence, cells were incubated for 24 h to establish mature E-cadherin junctions. After 24 h, the medium was exchanged in all wells, and then cells were subsequently treated with piperazine derivatives and washed with PBS prior to fixation. Cells were fixed at 4 °C in 4% formaldehyde and then permeabilized with 0.25% Triton for 15 min at 4 °C. E-cadherin junctions were stained with mouse anti-E-cadherin-Alexa 488 (BD Bioscience) at 1:50 in 2.5% BSA overnight at 4 °C. To boost the signal, additional rabbit anti-mouse antibody conjugated to Alexa-488 (Invitrogen) was diluted in 2.5% BSA at 1:200 and incubated on the slide for 1 h at room temperature. ZO1-594 (Thermo Fisher) was diluted 1:100 in 2.5% BSA and incubated on the slide at room temperature. Last, cells were stained with 10 mg/mL Hoescht 33342 at 1:10,000 dilution for 10 min in PBS at room temperature. In between each step, cells were washed three times with PBS.

Image Processing of Cell Junctions. For quantifying the area of cellular junctions, confocal images were taken on a Zeiss LSM 880 on a 40×, 1.2 NA oil immersion objective. Power, gain, and other relevant imaging parameters were kept identical in experiments where cells had the same passage number. Z-stacks were collected, and the maximum intensity projections were taken from each channel. For counting particles, a Gaussian filter of 2 pixels was applied to the nuclear Hoescht channel, and the images were thresholded. The "Analyze Particle" algorithm in ImageJ was utilized to count the number of nuclei in each field of view. At least 400 cells were imaged for each condition. In both the E-cadherin channel and ZO-1 channel, first, the "Subtract Background" algorithm was selected at 10 pixels. Then, both channels were thresholded, and the threshold was kept identical across images collected from the same experiment. Masks were defined for both the Ecadherin channel and ZO-1 channel, and the multiply function of the "Image Processing" algorithm was used in ImageJ to select only the region of the E-cadherin mask that was localized to the junction. Then, the area of each stain was measured and normalized to the entire area of the frame or to the number of cells in the frame.

Caco-2 Permeability Experiments. For transepithelial electrical resistance (TEER) and diffusion marker permeability experiments, an established model of rapid, 3-day Caco-2 intestinal epithelial monolayers was employed. ¹⁶ Briefly, Caco-2 cells were seeded on collagen-coated membrane supports for 24–48 h followed by addition

ACS Biomaterials Science & Engineering

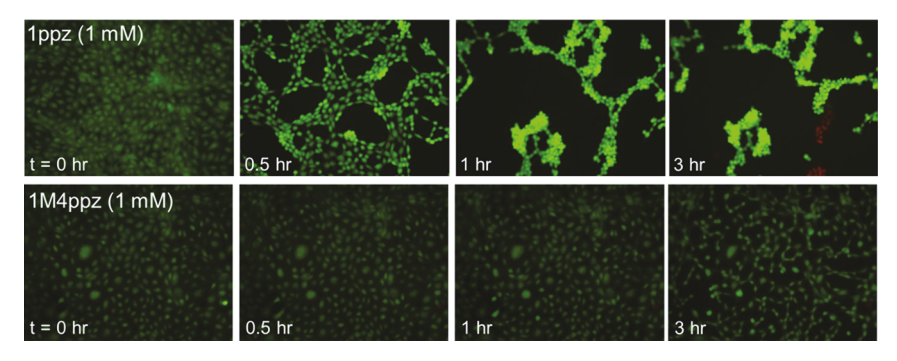


Figure 1. Addition of 1 mM piperazine derivatives to epithelial monolayers. NRK-52E epithelial cells were labeled with calcein AM (green) to image whole cells and propidium iodide (red) to show dead cells.

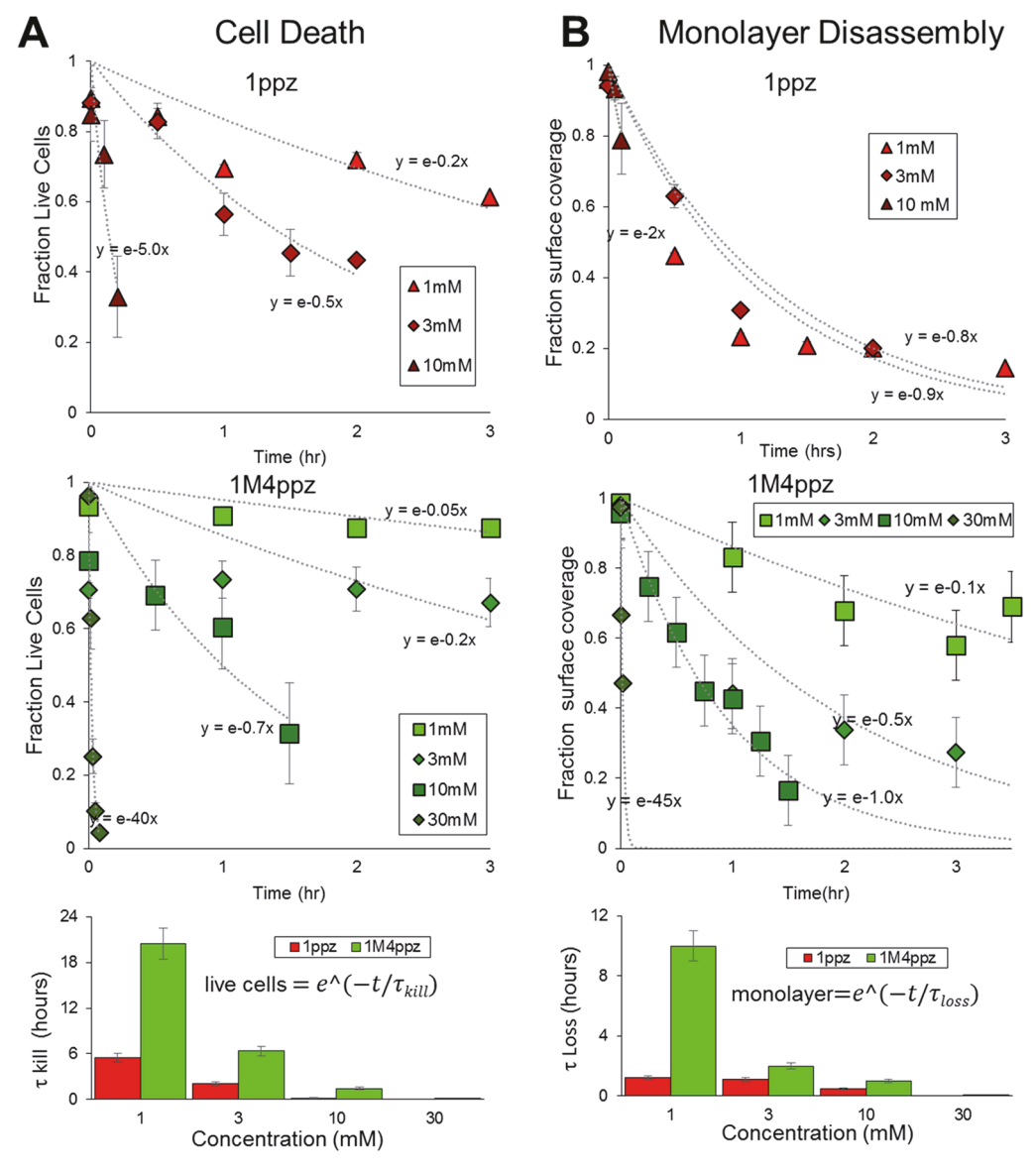


Figure 2. Concentration and time effects of 1ppz and 1M4ppz impact cell monolayers. (A) Cell toxicity, plotted as a fraction of live cells versus time, for NRK-52E cells is fit well by exponential decays. The exponential coefficients, τ_{kill} , are then plotted together for comparison. (B) Similarly, loss of cells from monolayer disassembly also fits as an exponential decay. The exponential coefficient τ_{loss} is plotted on a lower y axis than τ_{kill} since dead cells would also lead to monolayer disassembly.

to differentiation media and further incubation for 48 h. Initial TEER values of at least 150 $\Omega\cdot\text{cm}^2$ were used for experiments.

Inhibitor experiments in Caco-2 were performed as previously described. Briefly, calcein (0.5 mM) and varying concentrations (3, 10,

and 30 μ M) Y-27632 (Abcam) were added to the apical chamber and incubated for 1 h to obtain baseline TEER and permeability values. Piperazine treatments were added to the apical chambers at time 0, with negative control wells remaining in just media with calcein. TEER

readings were expressed as the ratio of a monolayer's resistance to initial resistance further normalized to the same ratio for the untreated control wells on the plate.

After 3 h, basal chamber medium fluorescence was measured at 495/515 nm (calcein) using a BioTek Synergy2 automated plate reader. Application of calibration curves yielded mass transferred across each monolayer, which was used in the permeability equation $P_{\rm app} = \frac{\Delta M}{C_a \Delta \Delta t}$, where $P_{\rm app}$ is the apparent monolayer permeability, ΔM is the marker mass, $C_{\rm a}$ is the apical marker concentration, A is the monolayer area, and Δt is the time.

RESULTS

Epithelial Monolayers Are Disrupted by Piperazine Derivatives. To investigate the disruptive effect of piperazine derivatives on cellular monolayers, NRK-52E epithelial cells were grown to monolayer confluence, and high concentrations of 1-phenylpiperazine (1ppz) or 1-methyl-4-piperazine (1M4ppz) were added to cells. Cells were imaged at 5 min intervals for 3 h with a combination of calcein AM to show all cells and propidium iodide (PI) to show dead cells (Figure 1). At a similar concentration (1 mM in Figure 1), 1ppz showed a more rapid dissociation of the monolayer structure, and dead cells were observed after 3 h. 1M4ppz showed slower dissociation of the monolayer and only a few dead cells after 3 h. In both cases, some cell attachments remained, resulting in elongated structures rather than cellular islands.

To quantify toxicity, we added 1, 3, 10, and 30 mM of 1ppz or 1M4ppz to monolayers of NRK-52E and measured PI-positive cells and all cell nuclei (by Hoechst 33342). Plots of the temporal decrease in fraction of live cells all fit to exponential decays. These kill curves show that, at all concentrations, 1M4ppz was three times less toxic; it would take at least three times as long for the same concentration 1M4ppz to kill cells as 1ppz (Figure 2A). Similarly, the rates by which the epithelial cells were lost from the surface, as measured by calcein dye, were also well fit by an exponential decay (Figure 2B).

In comparing cell death (τ_{kill}) and loss from monolayer disassembly (τ_{loss}) , 1ppz and 1M4ppz behaved differently, particularly at higher drug concentrations. 1M4ppz had a lower τ_{loss} than τ_{kill} at every treatment concentration, consistent with the fact that monolayer disruption is due to cellular disassembly. Conversely, 1ppz at 3 mM showed similar τ_{loss} and τ_{kill} , and at 10 mM, τ_{kill} is less than τ_{loss} , suggesting that cells are killed before they come apart. For future studies, we were interested in pursuing concentrations in which monolayers remained intact.

Fluctuation of Actin Structures by Piperazine. At lower concentrations, we considered the impact of piperazine derivatives on subcellular structures. We treated cells for 1 h with varying concentrations of 1ppz or 1M4ppz, fixed the cells, and imaged E-cadherin, tight junctions, and nuclei (Figure 3). We then considered primarily 1M4ppz at 0.1 and 0.5 mM for up to 1 h since, at this concentration and time frame, we could be sure the epithelial structure was completely maintained.

Cells were transiently transfected with RFP-tagged LifeAct so that only a sparse number of cells expressed the red actin-binding protein. Imaging these cells in a confluent monolayer treated with 1M4ppz showed a unique, high-resolution transient phenotype. Within a few minutes after treatment with 0.5 mM 1M4ppz, we observed a contraction of the cells, followed by recovery to normal levels (Figure 4A). Control monolayers and monolayers treated with 0.1 mM 1M4ppz showed a gradual area decrease in cells over time, likely associated with photobleaching of the edges (Figure 4B). In a separate experiment, we confirmed

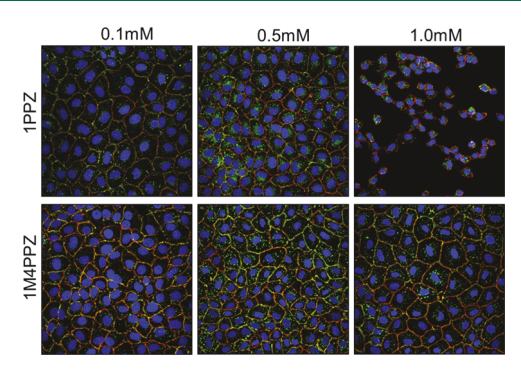


Figure 3. Imaging of cadherins and tight junctions in monolayers treated by piperazine. NRK-52E cells treated for 1 h with three concentrations of 1ppz or 1M4ppz show intact monolayer structures including right junctions (red, ZO-1), cadherins (green, E-cadherin), and regularly spaced nuclei (blue, Hoechst 33342). At 1 mM, 1ppz disrupts monolayers.

that the cell-cell junctions (Figure 4C) and actin stress fibers (Figure 4D) were intact in cells treated with 0.5 mM 1M4ppz.

Piperazine Derivatives Increase Intracellular Cellular Force Generation. Since we observed the dramatic initial contraction of cells with the added 1M4ppz, we hypothesized that piperazine increased the intracellular force. To measure changes in intracellular forces, we utilized our newly developed technique of sensors from intranuclear kinetics (SINK) by which fluctuations of chromatin-bound probes yield measurements of cellular force in the NRK-52E cell monolayer with the process mentioned in Experimental Materials and Methods, the mean squared displacement (MSD) of GFP-UBF1 spots (Figure 5A). The slopes of the MSD versus lag time are indicative of the force generated in the cell (Figure 5B). Unfortunately, 0.1 mM 1M4ppz shows a slightly nonlinear response, which may be a superposition of the cellular response to the drug and the time frame of the measurement. Still, both 0.1 mM 1M4ppz and 0.05 mM 1ppz show increased intracellular cell forces after treatment.

Piperazines Modify Subcellular Distribution of Junctional Proteins E-Cadherin and Tight Junctions. Increased actin—myosin force generation within the cell would manifest on a multicellular system by perturbing actin-associated cell—cell structures: the cadherin junctions. E-cadherin is the epithelial cadherin junction that interconnects cells. Conversely, tight junctions also connect epithelial cells within a monolayer, but these junctions are not cytoskeletally associated.

Consistent with this, we imaged both E-cadherins and tight junctions (by labeling ZO-1) by immunocytochemistry in fixed cells at 4 and 8 h after treatment with 1M4ppz (Figure 6A,B). At 8 h, there was a visible and statistically quantifiable reduction in E-cadherins but not tight junctions. Similarly, we treated monolayers with 1M4ppz or 1ppz at increasing concentrations for short times (>1 h). For both 1M4ppz and 1ppz, we observed a loss of E-cadherins at lower concentrations than tight junctions (Figure 6C). Specifically, for 1M4ppz, tight junctions remained at control levels at every concentration tested, but E-cadherin was slightly reduced at 0.5 and 1.0 mM with a statistically significant reduction in E-cadherin at 10 mM. For 1ppz, Ecadherins were statistically reduced from control at every concentration in a dose-dependent manner. In contrast, tight junctions were reduced from control only at 1.0 mM (the highest level tested by this method).

Piperazine-Induced Permeability in Caco-2 Cells Is Reduced with Myosin Motor Inhibitor. To test the

ACS Biomaterials Science & Engineering

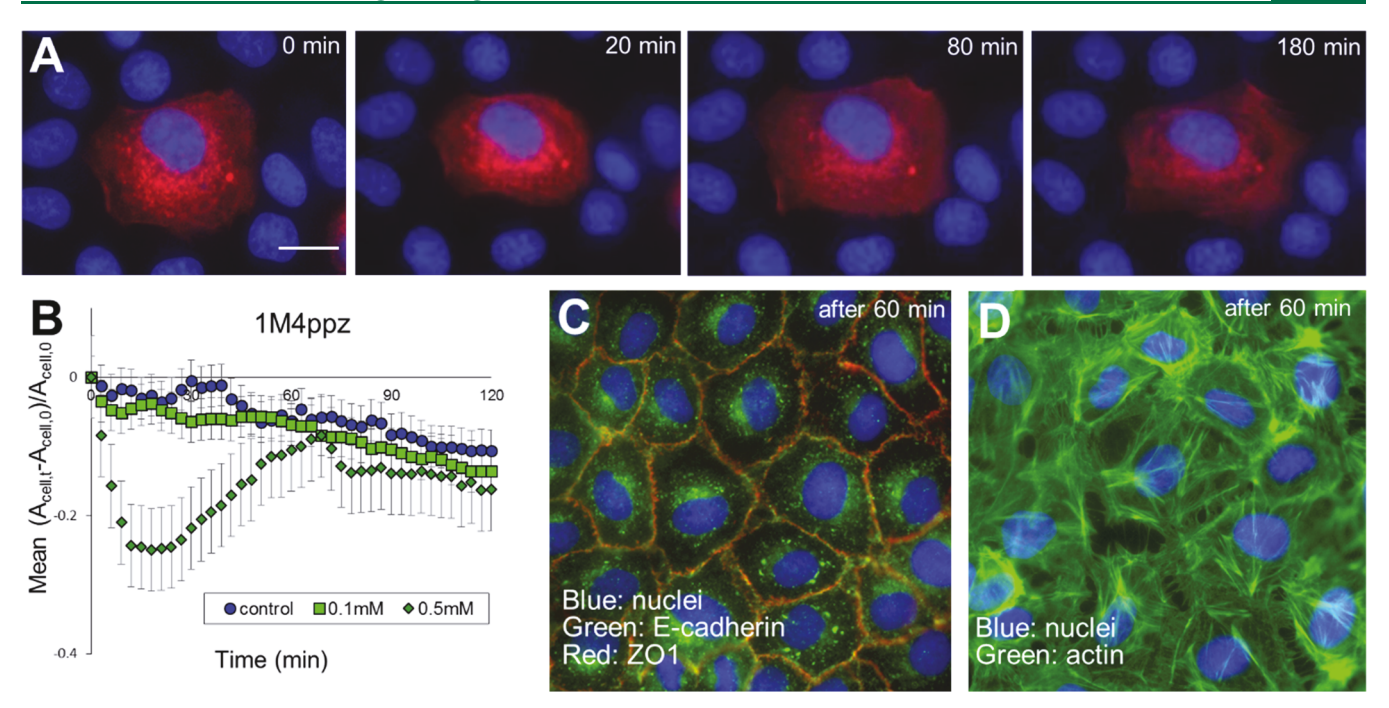


Figure 4. Transient cellular contraction with 0.5 mM 1M4ppz in NRK-52E cells. (A) Image sequence of cell transiently transfected with LifeAct-labeled actin that shows contraction and expansion after treatment with 0.5 mM 1M4ppz within a monolayer of cells imaged by blue nuclei (scale bar is 5 μ m). (B) Average projected area fraction change of transfected cells over time in the cell monolayer. (C, D) After 60 min of 0.5 mM 1M4ppz treatment, cell—cell junctions (C) and actin stress fibers (D) are intact.

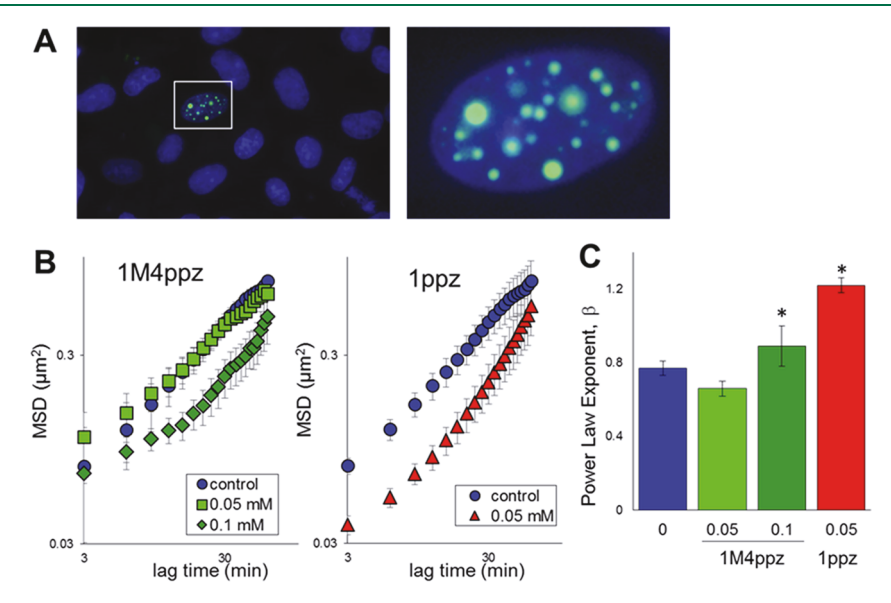


Figure 5. Increased intracellular forces after treatment of monolayer by 1ppz or 1M4ppz by SINK. (A) Particle tracking of subnuclear fluctuations of GFP-UBF1 in cells of confluent monolayers provides mean squared displacement (MSD) of particles versus lag time. (B) Comparisons of MSD to control NRK-52E on a log—log scale reveal changes in a power-law slope related to the force generation within cells. (C) The power-law exponent b is related to force generation. The increase in b for 0.1 mM 1M4ppz and 0.05 1ppz shows an increased actin—myosin-based force generation caused by the drug treatment.

hypothesis that epithelial permeability is a function of myosin motor activity, we examined permeability through Caco-2 intestinal epithelial cells. These cells form definitive apical and basal regimes as well as extremely strong junctions, although their culture restricts live-cell intracellular imaging. Myosin motor activity was inhibited using Y-27632, a cell-permeable selective inhibitor of ROCK (Rho-associated protein kinase), which is directly upstream of myosin phosphorylation and contraction. We examined membrane permeability to electro-

lytes through transepithelial electrical resistance (TEER; Figure 7A) and small molecules by measuring calcein permeability by a fluorescence plate reader (Figure 7B). In both cases, Caco-2 cells were treated with 6 mM 1ppz, which we previously showed to be efficacious in increasing epithelial permeability. This can be seen by the reduction in TEER reading (Figure 7A, red line) to under 25% of the control after 3 h and an increase in calcein permeability through the monolayer (Figure 7B) by 11-fold. Adding the ROCK inhibitor Y-27632, which reduces myosin

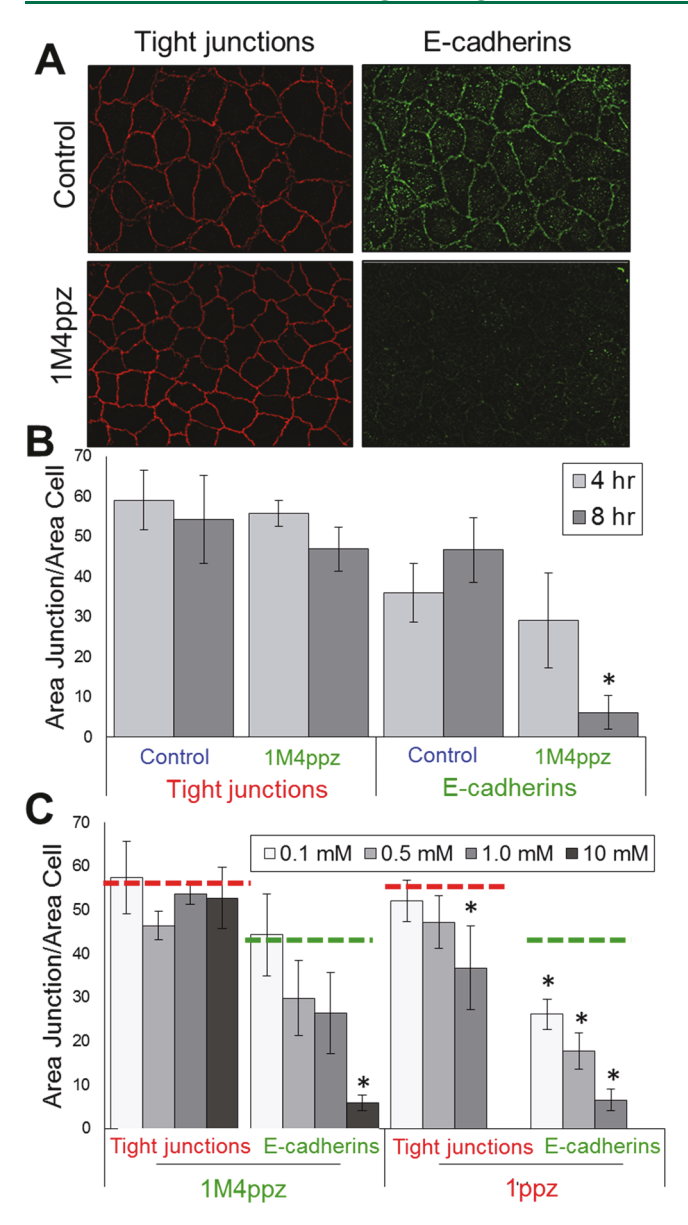


Figure 6. Cell junctions after treatment with piperazine derivatives. (A) Similar imaging conditions of either tight junctions (red, ZO-1) or Ecadherins (green) show differential reduction after treatment with 0.1 mM 1M4ppz versus the 0.5% DMSO control after 8 h. (B) Quantification of this low concentration for a long time is shown to be statistically significant at 8 h but not after 4 h. (C) Treatment with increasing concentrations at short times including 0.1, 0.5, and 1.0 mM for 1 h or 10 mM for 12 min shows reduction of E-cadherins. Treatments for 1 h of either drug at 10 mM resulted in a loss of all cells; at 12 min, no cells were present for 1ppz. The red and green dashed lines are the control levels of tight junctions and E-cadherins, respectively, from Figure 6. Error bars are standard deviation, and *p < 10^{-4} by Student's t test with DMSO control.

motor activity, rescued monolayer permeability both by TEER and calcein permeability. Interestingly, calcein permeability is more dramatically impacted by Y-27632. This may suggest that inhibition of myosin motor activity regulates movement of larger molecules (MW \approx 100–1000 g/mol) compared with electrolytes (MW \approx 10 g/mol).

DISCUSSION

Epithelial Monolayers Are Disrupted by Piperazine Derivatives. In terms of the ability to increase the permeability of an epithelial monolayer, both 1ppz and 1M4ppz disrupt the cell monolayer. However, with high concentrations (3, 10, and 30 mM), NRK-52E epithelial cell monolayers were disrupted, and cell death occurred. 1M4ppz caused primarily cellular disassembly ($\tau_{\rm loss} > \tau_{\rm kill}$ at every concentration). However, 1ppz at higher concentrations killed cells faster than cellular disassembly ($\tau_{\rm kill} \approx \tau_{\rm loss}$ and $\tau_{\rm kill} > \tau_{\rm loss}$). 1ppz treatment generated more dead cells and created intracellular gaps much faster than the cell monolayer with same concentration of 1M4ppz treatment. This result is also consistent with the previous study showing that 1M4ppz has much lower toxicity potential and relatively lower enhancement potential than 1ppz.⁷

Impacts of Piperazines on Different Epithelial Cell Types Moving in Situ. In comparing toxicity data of 1ppz and 1M4ppz on NRK-52E epithelial cells to studies with Caco-2 cells, it is apparent that piperazines cause differing degrees of toxicity between the two cell lines. For the studies here, we use 0.05-0.5 mM 1ppz for NRK-52E cells and 6 mM 1ppz for Caco-2 cells to show similar changes to the monolayer function. Caco-2 cells are human epithelial colorectal adenocarcinoma cells that can be grown on double-sided substrates to form apical and basal regions that mimic the gastrointestinal tract. Conversely, NRK-52E cells are rat kidney epithelial cells that form epithelial junctions and robust cytosketetal structures. At first glance, it would make sense that Caco-2 cells would be a better option to mimic the toxicity of piperazines for intestinal epithelia. However, a previous study directly examining 1ppz on Caco-2 cells and rat intestinal mucosae showed that 1ppz had an LD₅₀ (median lethal dose) of 60 mM on the Caco-2 cells, whereas 1 mM 1ppz showed obvious cellular defects in the mucosa with large tissue-wide death by 10 mM 1ppz.8 Thus, it may not be clear which cell type is appropriate for testing the efficacy for epithelial permeability. Transepithelial electrical resistance (TEER) assays require cell types that possess a strong barrier function such as Caco-2 cells. However, cells of the mucosa appear to be likely more prone to death and tissue disruption with permeabilization agents than cultured Caco-2 cells. This may be, in part, due to the force generation observed here. We suggest using a complement of cell types to fully understand mechanisms of permeation enhancement in vitro. As an extension of these results to animal studies, our (Whitehead) work has found that 1ppz is dosed at 60 mg/kg in mice (~200 mM per delivery volume) to achieve an 11-fold increase of a 4 kDa fluorescein molecule after 4 h (data not shown). This dose is many-folds higher than that used here for cell culture studies. While we anticipate that the mechanism of action will be the same or similar in animals as we report here, additional work would be needed to confirm these findings.

Piperazine Derivatives Increase Intracellular Force Generation. Guided by our imaging of cytoskeletal contraction after piperazine addition, we measured the increase in intracellular force generation using SINK. The addition of 0.1 mM 1M4ppz to the NRK-52E monolayer caused an ~15% increase in force generation, and the addition of 0.05 mM 1ppz caused an ~50% increase in force generation. Previous studies have shown that inhibition of myosin light chain kinase (MLCK), responsible for phosphorylating nonmuscle myosin II, with the compound ML9 (part of a class of napthalenesulfo-

ACS Biomaterials Science & Engineering

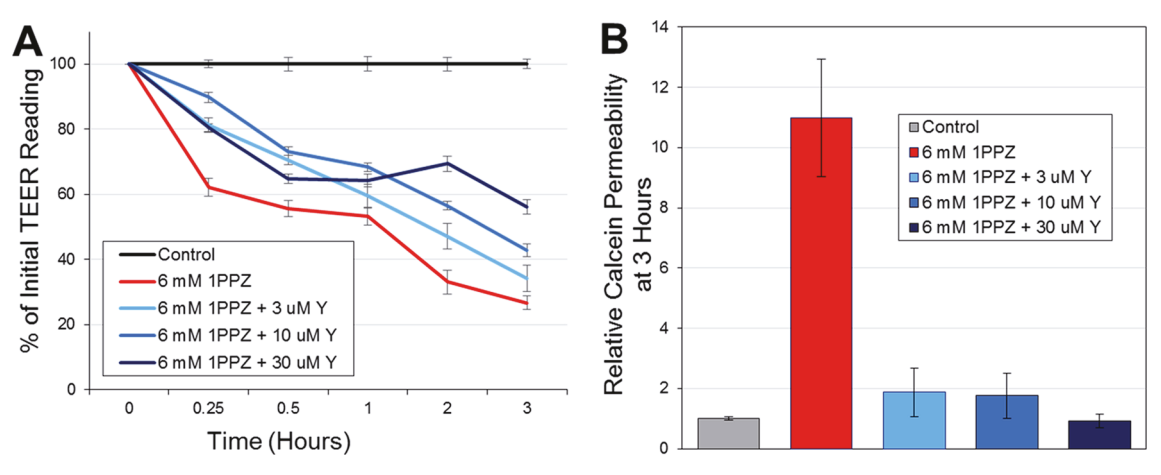


Figure 7. Permeability of Caco-2 epithelial cell monolayers by 1ppz reduced by myosin inhibitor Caco-2 cells grown and differentiated on Transwell plates to a TEER reading of at least $150 \,\Omega \cdot \mathrm{cm}^2$. Fluorescent calcein, $6 \,\mathrm{mM}$ 1ppz, and varying concentrations of Y-27632 were added to the apical wells of the cells. With the $6 \,\mathrm{mM}$ 1ppz, Caco-2 cells have increased permeability as shown in red by (A) transepithelial electrical resistance and (B) calcein permeability compared to the control, which has no 1ppz. The addition of increasing levels of Y-27632 shows an antagonistic effect of 1ppz permeability, consistent with the idea that inhibiting myosin motor activity reduces epithelial permeability.

namides including ML7, routinely used in cadherin and cytoskeletal studies 17,18) potently inhibits the permeabilizing effects of 1ppz, indicating that actin contractility plays a considerable role in the efficacy of permeation enhancers. Similarly, both in vivo 19 and in vitro 20 studies have demonstrated that successful assembly of cadherin junctions potentiate the assembly of tight junctions via coordination with α -catenin. Mislocalization or knockout of E-cadherin junctions can result in similar mislocalization of tight junctions 21 in epithelial cell types. Thus, our work showing that 1ppz- or 1M4ppz-induced increased cellular force generation by myosin that leads to a breakdown of cadherins and then tight junctions, ultimately causing cells to pull apart, is consistent with the body of epithelial cell work from the past two decades.

What Makes a Good Permeation Enhancer? Piperazine derivatives have been investigated for their ability to enhance intestinal permeability and increase pharmaceutical uptake of large molecules. Other permeation enhancers, such as chitosan, alter the distribution of actin cytoskeleton and may alter the long-term function of the tissue. 22 In this study, we show that piperazine derivatives increase force generation within cells and reorganize cadherins and eventually tight junctions. This role of mechanosensitivity in cells to form—or in this case, dissociate tight junctions by the way of actin-myosin forces through cadherins has recently been shown in generation of epithelial tissue.²³ We suggest that manipulation of this mechanism may be a highly effective method for transient monolayer permeability: increased cellular contraction would add strain to the monolayer and pull holes between cells or at least microdefects at cell-cell junctions. This would increase monolayer permeability with the addition of the drug. However, there would not be large gaps or dead cells. After the removal of the enhancer, cells would relax back to their initial state and reform the epithelial barrier. We argue that the generalized mechanism discovered here could be applicable to the development of other permeation enhancers. For example, other small molecules that have the ability to transiently activate cellular contraction would also be useful in facilitating permeation without promoting cell death.

CONCLUSIONS

We used a model epithelial cell line to visualize the subcellular changes associated with two piperazine derivatives that enhance epithelial monolayer permeability. We observe that these piperazine derivatives increase force generation in cells, leading to disruption of cadherin junctions and then tight junctions. Thus, cells are transiently stimulated to increase force generation and then alter cell—cell interactions, leading to tissue-level alterations of the structure.

ASSOCIATED CONTENT

S Supporting Information

The Supporting Information is available free of charge at https://pubs.acs.org/doi/10.1021/acsbiomaterials.9b01660.

Colocalization of ZO-1 and E-cadherin at different times after treatment with piperazine derivatives and concentrations similar to Figure 6 (PDF)

■ AUTHOR INFORMATION

Corresponding Author

*E-mail: krisdahl@cmu.edu.

ORCID 🧐

Kathryn A. Whitehead: 0000-0002-0100-7824

Kris Noel Dahl: 0000-0002-3874-1547

Author Contributions

S.Z. and K.L. contributed equally to this work. The manuscript was written through contributions of all authors. All authors have given approval to the final version of the manuscript.

Note

The authors declare no competing financial interest.

ACKNOWLEDGMENTS

Funding was provided by NSF grant numbers 1634888 (to K.N.D.) and 1807983 (to K.A.W.). K.L. was supported by NIH 5T32GM088119-08. N.G.L. was supported by NSF-GRFP DGE1252522. Any opinions, findings, and conclusions or recommendations expressed in this material are those of the author(s) and do not necessarily reflect the views of the National Science Foundation.

ABBREVIATIONS

1ppz, 1-phenylpiperazine; 1M4ppz, 1-methyl-4-phenylpiperazine; SINK, sensors from intranuclear kinetics; τ_{kill} , time scale from cell death; τ_{loss} , time scale from monolayer disassembly

REFERENCES

- (1) Moroz, E.; Matoori, S.; Leroux, J. C. Oral delivery of macromolecular drugs: Where we are after almost 100years of attempts. *Adv. Drug Delivery Rev.* **2016**, *101*, 108–121.
- (2) Aungst, B. J. Absorption enhancers: applications and advances. *AAPS J.* **2012**, *14*, 10–18.
- (3) Pan, Y.; Li, Y. J.; Zhao, H. Y.; Zheng, J. M.; Xu, H.; Wei, G.; Hao, J. S.; Cui, F. D. Bioadhesive polysaccharide in protein delivery system: chitosan nanoparticles improve the intestinal absorption of insulin in vivo. *Int. J. Pharm.* **2002**, 249, 139–147.
- (4) Leone-Bay, A.; Santiago, N.; Achan, D.; Chaudhary, K.; DeMorin, F.; Falzarano, L.; Haas, S.; Kalbag, S.; Kaplan, D.; Leipold, H. Nacylated alpha-amino acids as novel oral delivery agents for proteins. *J. Med. Chem.* **1995**, *38*, 4263–4269.
- (5) Salama, N. N.; Eddington, N. D.; Fasano, A. Tight junction modulation and its relationship to drug delivery. *Adv. Drug Delivery Rev.* **2006**, *58*, 15–28.
- (6) Gupta, V.; Hwang, B. H.; Doshi, N.; Mitragotri, S. A permeation enhancer for increasing transport of therapeutic macromolecules across the intestine. *J. Controlled Release* **2013**, *172*, 541–549.
- (7) Fein, K. C.; Lamson, N. G.; Whitehead, K. A. Structure-Function Analysis of Phenylpiperazine Derivatives as Intestinal Permeation Enhancers. *Pharm. Res.* **2017**, *34*, 1320–1329.
- (8) Bzik, V. A.; Brayden, D. J. An Assessment of the Permeation Enhancer, 1-phenyl-piperazine (PPZ), on Paracellular Flux Across Rat Intestinal Mucosae in Ussing Chambers. *Pharm. Res.* **2016**, 33, 2506–2516.
- (9) Pokorna, A.; Bobal, P.; Oravec, M.; Rarova, L.; Bobalova, J.; Jampilek, J. Investigation of Permeation of Theophylline through Skin Using Selected Piperazine-2,5-Diones. *Molecules* **2019**, *24*, 566.
- (10) Pappinen, S.; Tikkinen, S.; Pasonen-Seppänen, S.; Murtomäki, L.; Suhonen, M.; Urtti, A. Rat epidermal keratinocyte organotypic culture (ROC) compared to human cadaver skin: the effect of skin permeation enhancers. *Eur. J. Pharm. Sci.* **2007**, *30*, 240–250.
- (11) Lamson, N. G.; Cusimano, G.; Suri, K.; Zhang, A.; Whitehead, K. A. The pH of Piperazine Derivative Solutions Predicts Their Utility as Transepithelial Permeation Enhancers. *Mol. Pharmaceutics* **2016**, *13*, 578–585.
- (12) Saw, T. B.; Doostmohammadi, A.; Nier, V.; Kocgozlu, L.; Thampi, S.; Toyama, Y.; Marcq, P.; Lim, C. T.; Yeomans, J. M.; Ladoux, B. Topological defects in epithelia govern cell death and extrusion. *Nature* **2017**, *544*, 212–216.
- (13) Spagnol, S. T.; Dahl, K. N. Active cytoskeletal force and chromatin condensation independently modulate intranuclear network fluctuations. *Integr. Biol.* **2014**, *6*, 523–531.
- (14) Armiger, T. J.; Lampi, M. C.; Reinhart-King, C. A.; Dahl, K. N. Determining mechanical features of modulated epithelial monolayers using subnuclear particle tracking. *J. Cell Sci.* **2018**, *131*, jcs216010.
- (15) Booth-Gauthier, E. A.; Alcoser, T. A.; Yang, G.; Dahl, K. N. Force-induced changes in subnuclear movement and rheology. *Biophys. J.* **2012**, *103*, 2423–2431.
- (16) Gupta, V.; Doshi, N.; Mitragotri, S. Permeation of insulin, calcitonin and exenatide across Caco-2 monolayers: measurement using a rapid, 3-day system. *PLoS One* **2013**, 8, No. e57136.
- (17) Borghi, N.; Sorokina, M.; Shcherbakova, O. G.; Weis, W. I.; Pruitt, B. L.; Nelson, W. J.; Dunn, A. R. E-cadherin is under constitutive actomyosin-generated tension that is increased at cell-cell contacts upon externally applied stretch. *Proc. Natl. Acad. Sci. U. S. A.* **2012**, *109*, 12568–12573.
- (18) Reig, J. A.; Viniegra, S.; Ballesta, J. J.; Palmero, M.; Gutierrez, L. M. Naphthalenesulfonamide derivatives ML9 and W7 inhibit catecholamine secretion in intact and permeabilized chromaffin cells. *Neurochem. Res.* 1993, 18, 317–323.

- (19) Tunggal, J. A.; Helfrich, I.; Schmitz, A.; Schwarz, H.; Günzel, D.; Fromm, M.; Kemler, R.; Krieg, T.; Niessen, C. M. E-cadherin is essential for in vivo epidermal barrier function by regulating tight junctions. *EMBO J.* **2005**, *24*, 1146–1156.
- (20) Maiers, J. L.; Peng, X.; Fanning, A. S.; DeMali, K. A. ZO-1 recruitment to alpha-catenin–a novel mechanism for coupling the assembly of tight junctions to adherens junctions. *J. Cell Sci.* **2013**, *126*, 3904–3915.
- (21) Campbell, H. K.; Maiers, J. L.; DeMali, K. A. Interplay between tight junctions & adherens junctions. Exp. Cell Res. 2017, 358, 39–44.
- (22) Ranaldi, G.; Marigliano, I.; Vespignani, I.; Perozzi, G.; Sambuy, Y. The effect of chitosan and other polycations on tight junction permeability in the human intestinal Caco-2 cell line(1). *J. Nutr. Biochem.* **2002**, *13*, 157–167.
- (23) Rübsam, M.; Mertz, A. F.; Kubo, A.; Marg, S.; Jüngst, C.; Goranci-Buzhala, G.; Schauss, A. C.; Horsley, V.; Dufresne, E. R.; Moser, M.; Ziegler, W.; Amagai, M.; Wickström, S. A.; Niessen, C. M. E-cadherin integrates mechanotransduction and EGFR signaling to control junctional tissue polarization and tight junction positioning. *Nat. Commun.* **2017**, *8*, 1250.